

“© 2025 IEEE. Personal use of this material is permitted. Permission from IEEE must be obtained for all other uses, in any current or future media, including reprinting/republishing this material for advertising or promotional purposes, creating new collective works, for resale or redistribution to servers or lists, or reuse of any copyrighted component of this work in other works.”

Ultra-Wideband Vertically Polarized Circular Array for Passive Sensing Applications

Gengming Wei¹, Yi He¹, Richard W. Ziolkowski², Y. Jay Guo¹

¹ Global Big Data Technologies Centre, University of Technology Sydney, Sydney, Australia, gengming.wei@student.uts.edu.au

² Department of Electrical and Computer Engineering, University of Arizona, Tucson, USA, ziolkows@arizona.edu

Abstract— We present an ultra-wideband (UWB) vertically polarized long-slot circular phased array with a compact design for passive sensing applications. Unlike conventional tightly coupled cylindrical systems that require multiple circular arrays, our quasi-magnetic current sheet array uses a single circular array while achieving similar radiated field properties. A 16-element prototype demonstrates azimuthally invariant radiation capabilities. Measurements indicate that the array offers wide impedance bandwidth, high cross-polarization discrimination (XPD), and significant compactness. In its omnidirectional mode, the array achieves a 107.07% bandwidth ($VSWR \leq 2.0$) with XPD better than 19.5 dB. In its directional mode, it operates over 100% bandwidth with XPD better than 20.9 dB. The prototype also exhibits excellent azimuthal out-of-roundness (better than 1.3 dB in its omnidirectional mode) and scan-invariant radiation with a maximum deviation of only 0.8 dB in its directional mode.

Index Terms— Circular phased array, directional radiation, long-slot array, omnidirectional radiation, ultra-wideband (UWB), vertical polarization (VP).

I. INTRODUCTION

Next-generation wireless communication systems are progressing toward enhanced intelligence and multifunctionality [1], [2]. In addition to providing high-speed and ultra-reliable communications, these systems are expected to integrate sensing functionalities that improve quality of life through applications such as traffic monitoring, disaster prediction, and health diagnostics (such as fall detection). Within this context, Passive Sensing (PS) systems have become a significant focus due to their capability to operate without transmitting their own signals. By utilizing existing signals from current wireless infrastructures—including broadcast services, cellular base stations, satellites, and Wi-Fi networks—PS systems offer advantages such as cost reduction and decreased electromagnetic interference [3]. As illustrated in Fig. 1, PS systems that receive and process multiband signals from modern wireless infrastructures can deliver low-power, non-intrusive solutions for environmental sensing, target recognition at multiple scales, data analysis, and monitoring.

Advancements in PS systems have stimulated the desire for advanced antenna designs, especially in bandwidth, beam steering flexibility, and polarization diversity. This demand arises from their need to receive multiband signals from various directions. Ultra-wideband (UWB) circular phased arrays are particularly appealing because they provide scan-invariant azimuthal beams over broad frequency ranges,

making them ideal for integration with modern wireless systems across diverse bands.

A key design challenge for UWB circular arrays is selecting radiating elements that achieve the desired polarization while maintaining compactness. The tightly coupled current sheet array approach has emerged as a promising solution for achieving wide bandwidths [4], [5], [6], [7]. Compared to using frequency-independent antennas as array elements, UWB current sheet arrays are more compact [3], [8], [9], [10]. While this method has been successfully applied to UWB 2D planar arrays and horizontally polarized (HP) circular arrays, e.g., [11], [12], [13], its extension to UWB vertically polarized (VP) circular arrays presents unique challenges due to the difficulty in establishing the required tight coupling effects [14], [15], [16].

This paper introduces an innovative method to achieve UWB performance in a compact VP circular phased array whose elements are tightly coupled. The developed design employs a single circular array instead of the multiple stacked arrays typically used in UWB VP cylindrical arrays. The developed single-layer UWB VP circular array offers several advantages over prior designs: a broad impedance bandwidth exceeding 100% in both its omnidirectional ($VSWR \leq 2$) and directional ($VSWR \leq 3$) modes; a significantly more compact design with reduced element height and radial length; excellent azimuthal out-of-roundness; and improved cross-polarization discrimination (XPD) levels. A prototype array was fabricated and tested; the measured results closely match its simulated performance characteristics.

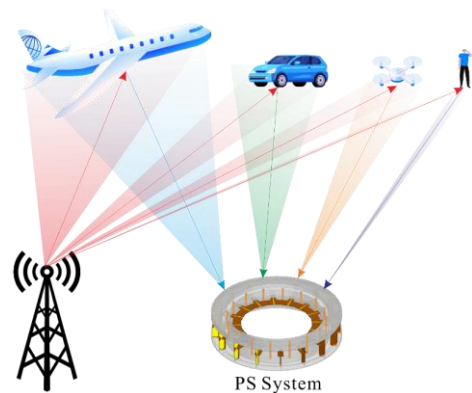


Fig.1. Operational scenario for passive sensing systems utilizing existing ground-based signals.

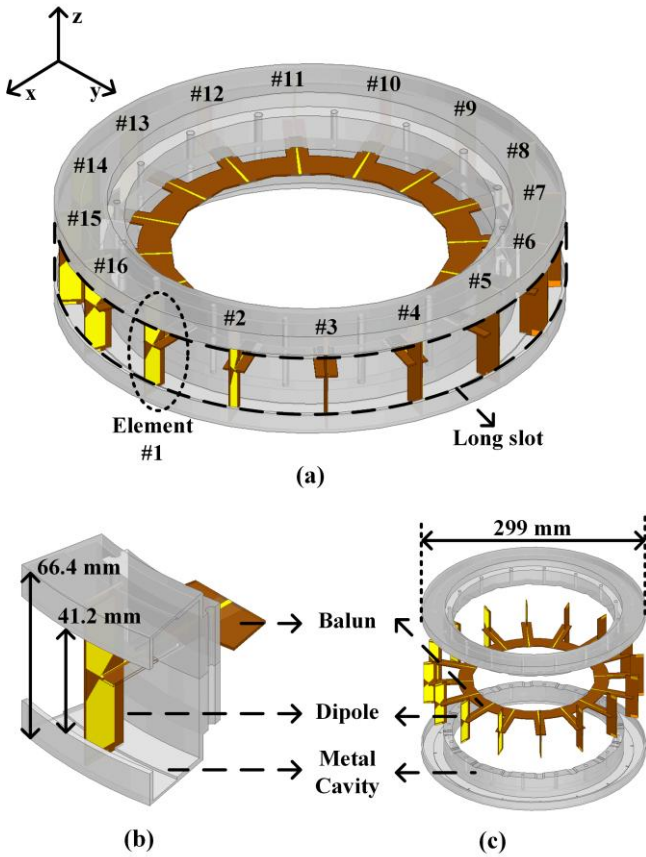


Fig.2. The developed UWB VP circular array. (a) Isometric view. (b) Enlarged view of its unit cell. (c) Exploded-view.

II. ARRAY DESIGN

A. Antenna Structure

Fig. 2 details the developed 16-element ultra-wideband (UWB) vertically polarized (VP) circular phased array. An isometric view is shown in Fig. 2(a), where the elements are numbered counterclockwise starting from element #1 located on the positive x-axis. Dashed lines indicate both the unit cell of the array—represented by element #1 in Fig. 2(b)—and an outline of the effective long circumferential slot. The array is comprised of three main components: an open metal cavity forming the circumferential slot as the primary radiating area, 16 dipole elements that excite a continuous magnetic current along this slot, and 16 UWB tapered baluns for feeding.

The dimensions of the main components and overall size are detailed in Figs. 2(b) and 2(c). The array has a diameter of 299.0 mm and a height of 66.4 mm. The circumferential slot is 41.2 mm wide accounts for 62.0% of the array's height. The metal cavity was fabricated from an aluminum alloy using standard machining techniques. The dipoles and baluns were constructed on copper-clad RT/Duroid 5880 substrates (1.016 mm thick, 0.5 oz copper, and relative permittivity $\epsilon_r = 2.2$).

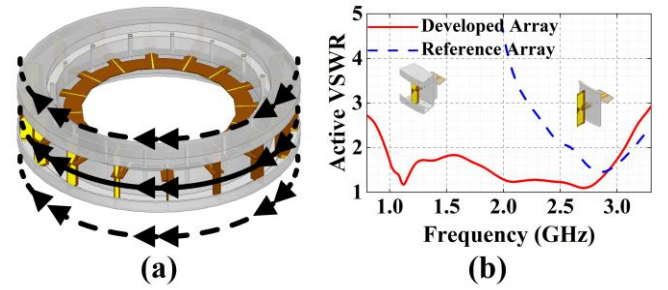


Fig.3. Operating principle and bandwidth restoration of the developed array. (a) Illustration of the magnetic current sheet. (b) Comparison of the simulated VSWR values of the developed array and the reference array (long slot and side walls removed) as functions of the source frequency.

B. Achieving Its UWB Bandwidth

A critical property of a current sheet array is that it functions as an array of continuous elements on a unique aperture, rather than as an array of independent discrete radiating elements [14], [15], [16]. In conventional arrays of resonant antennas, mutual coupling is generally considered detrimental because it can degrade impedance matching. However, high mutual coupling in the context of current sheet arrays is advantageous for achieving ultra-wideband (UWB) performance [7].

As shown in Fig. 3(a), vertically polarized (VP) dipoles are used to excite continuous magnetic currents along a long circumferential slot. This configuration can be conceptualized as a linear array of interconnected magnetic dipoles. By the principle of duality, it is analogous to a linear array of connected electric dipoles, as previously reported in horizontally polarized (HP) circular array studies [11], [12], [13]. It is important to note that wideband performance is constrained when the dipoles are connected and replicated in only one dimension [5]; a two-dimensional (2D) array is often required to achieve improved impedance matching.

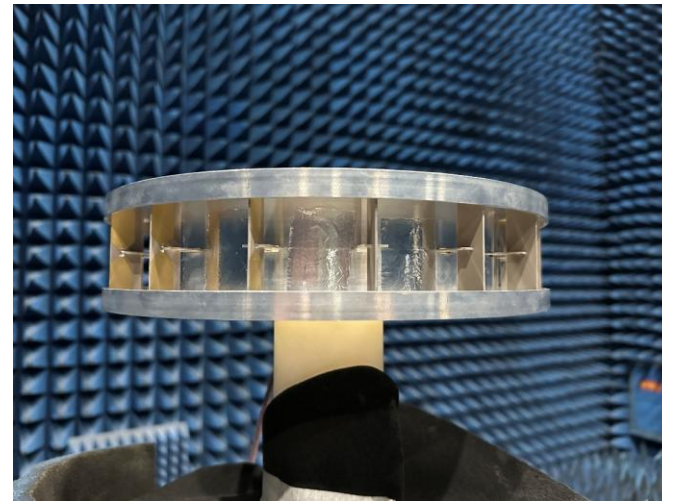


Fig. 4. Fabricated array prototype under test in the anechoic chamber.

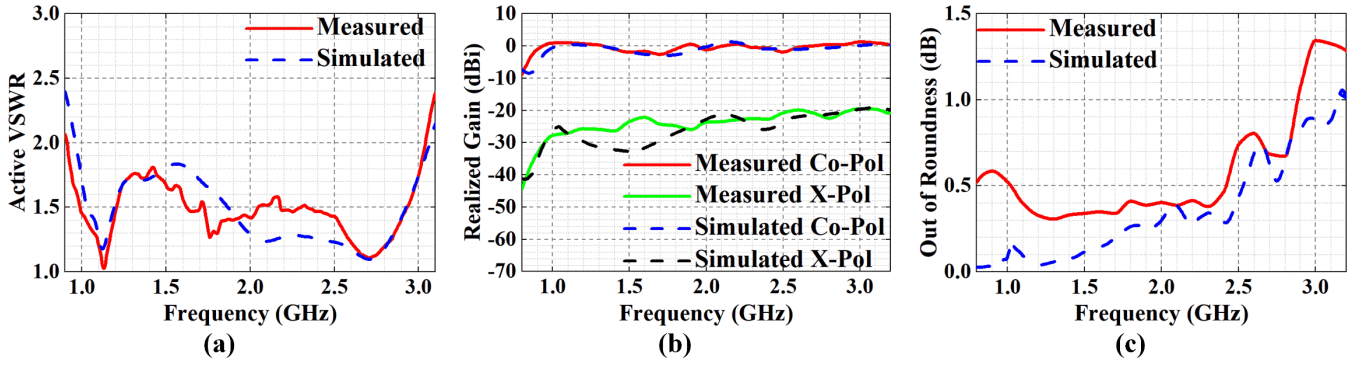


Fig. 5. Measured and simulated results of the developed array in the omnidirectional mode including (a) active VSWR of element #1, (b) realized gain of co-pol and x-pol, and (c) out of roundness of co-pol in horizontal plane.

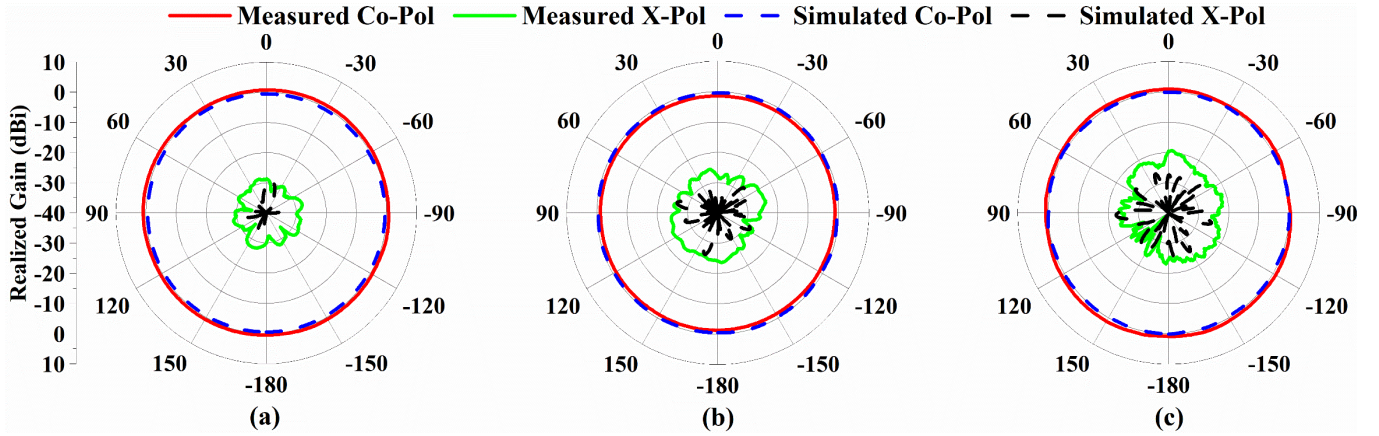


Fig. 6. Measured and simulated realized gain patterns in the horizontal plane of the prototype in its omnidirectional mode at (a) 1.0, (b) 2.0, and (c) 3.0 GHz.

This explains why reported UWB VP circular arrays [14], [15] utilize frequency-independent antennas as their radiating elements rather than dipoles, i.e., it is challenging to realize a VP current sheet with only one circular array.

To address this issue, horizontal metal walls are incorporated at both ends of the vertically oriented dipoles, as illustrated in Fig. 1. These walls act as perfect electric conductors (PEC), creating mirrored magnetic currents alongside the original ones. This configuration forms a quasi-magnetic current sheet array using a single circular array, thereby enhancing the UWB performance and minimizing its physical size. Fig. 3(b) compares the simulated VSWR values of the developed array with that of a reference array (the same array without the horizontal plates and side walls) across the same frequency range. The results show that removing the long slot and side walls significantly deteriorates the impedance performance.

III. DESIGN VERIFICATION

To validate the antenna design and its performance, a 16-element array with a radius of 149.5 mm was fabricated and measured. This size choice balanced performance and cost considerations. Fig. 4 shows the fabricated prototype in the anechoic chamber. Both the active VSWR and far-field

radiation patterns were measured.

A. Omnidirectional Mode Performance

Fig. 5(a) presents the active VSWR of the array in its omnidirectional mode, demonstrating the achievement of ultra-wideband (UWB) bandwidth. The measured (simulated) active impedance bandwidth with $VSWR \leq 2.0$ is 107.07% (103.96%), spanning from 0.92 (0.97) to 3.04 (3.07) GHz. The results showed good agreement with their simulated values with only minor discrepancies attributed to fabrication and measurement tolerances.

Fig. 5(b) displays the realized gain in the horizontal plane. The measured and simulated co-polarized gains remain relatively stable around 0 dBi. The measured and simulated cross-polarization discrimination (XPD) levels are better than 19.5 and 19.6 dB, respectively. The slight variations between them are ascribed to measurement errors and insertion losses from the power divider and feed lines.

Fig. 5(c) shows the out-of-roundness values of the far-field patterns versus frequency. The omnidirectional performance is robust across the entire operating bandwidth, with measured and simulated maximum out-of-roundness values of 1.3 dB and 0.9 dB, respectively.

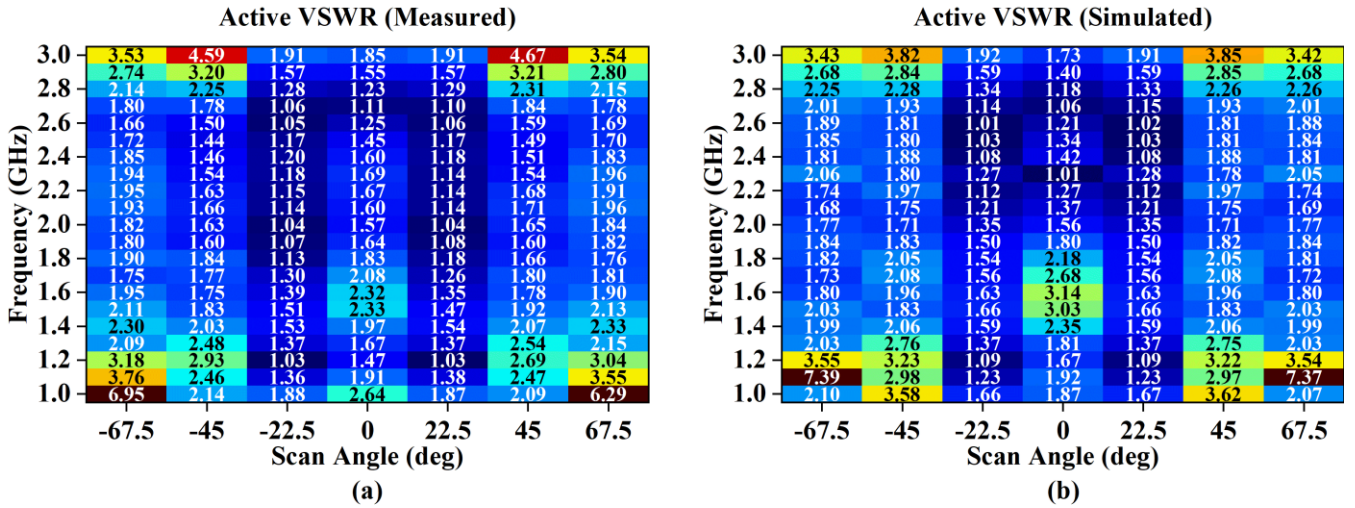


Fig. 7. Measured and simulated active VSWR of element #1 of the prototype at different scan angles in its directional mode. (a) Measured active VSWR. (b) Simulated active VSWR.

Fig. 6 provides the measured and simulated horizontal-plane realized gain patterns of the array in its omnidirectional mode at representative frequencies of 1.0, 2.0, and 3.0 GHz. Uniform omnidirectional performance is observed at all frequencies.

B. Directional Mode Performance

Fig. 7 displays the measured and simulated active VSWR distribution maps for element #1 in the array's directional mode as functions of scan angle and frequency. The VSWR values vary with the scan angle and are relatively symmetric about the beam direction. Despite the array's compact size, a VSWR less than 3.0 is observed across most of the map, except at the low- and high-frequency ends when the scan angle deviates significantly from the normal direction.

Fig. 8(a) shows the measured and simulated realized gains of the array in its directional mode when the beam is directed

at 0° . The co-polarized realized gain exhibits a progressive upward trend with a measured (simulated) peak gain of 12.2 (11.1) dBi within the operating band. The measured (simulated) broadside XPD levels exceed 20.9 (29.7) dB. Minor discrepancies between the measured and simulated values are primarily due to fabrication and measurement precision, including errors associated with the reference antenna. Fig. 8(b) presents the realized gain as a function of frequency and scan angle. The measured (simulated) maximum deviation is 0.8 (0.6) dB, demonstrating the array's ability to provide scan-invariant horizontal patterns in its directional mode.

To further understand the directional performance, Fig. 9 presents the measured and simulated realized gain patterns in directional mode at 1.0, 2.0, and 3.0 GHz. Due to the scan-invariant characteristic of the circular array, only patterns pointed at 0° are shown for clarity. The measured and

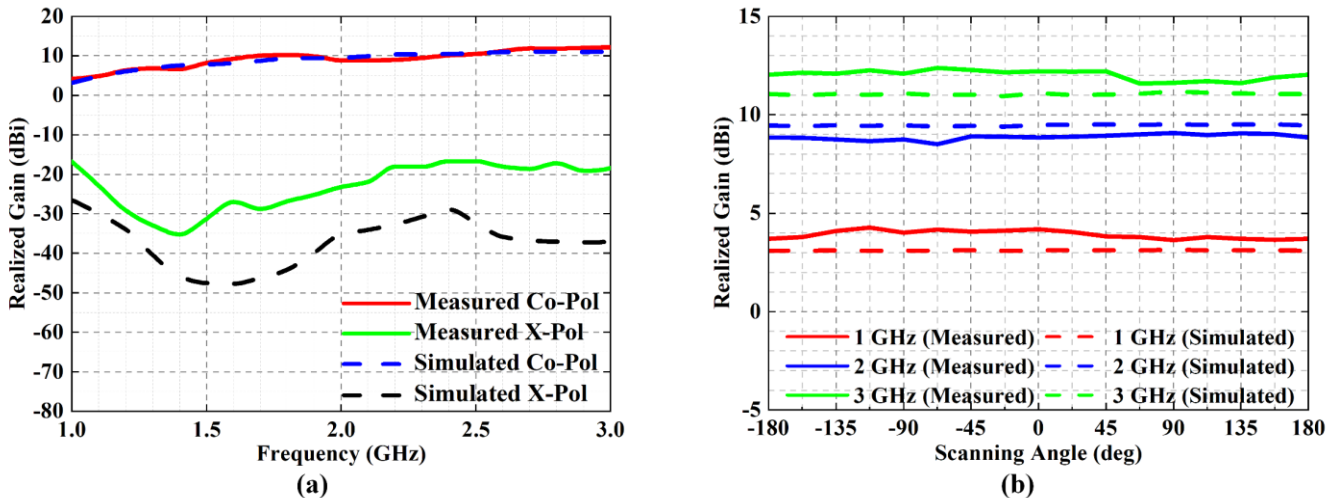


Fig. 8. Measured and simulated results of the prototype in its directional mode. (a) Realized gain of the beam directed at 0° . (b) Realized gain of its beam as a function of the scan angle for different frequencies.

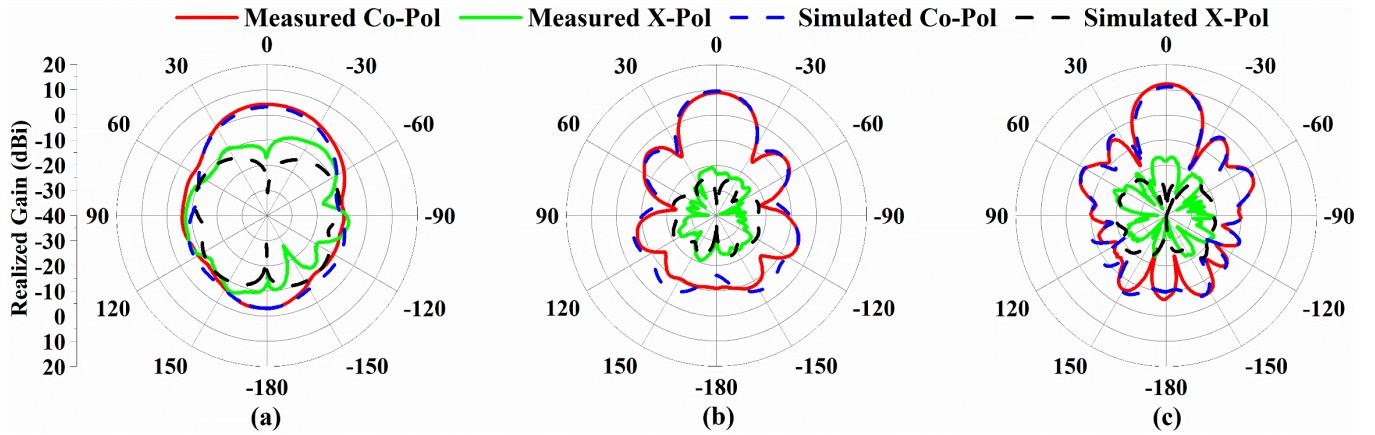


Fig. 9. Measured and simulated realized gain patterns at (a) 1.0, (b) 2.0, and (c) 3.0 GHz, when the beam is directed towards 0°.

simulated co-polarized results agree well, with broadside XPD levels exceeding 20.9 dB in both cases.

IV. CONCLUSION

A compact ultra-wideband (UWB) vertically polarized (VP) long-slot circular phased array was presented. Unlike previously reported UWB circular arrays, this VP design generates a quasi-magnetic current sheet along a long circumferential slot to achieve UWB property. The design requires only a single circular array, unlike the multiple stacked circular arrays typically used in cylindrical arrays. A 16-element prototype was fabricated and measured, demonstrating azimuthally invariant radiation characteristics. In its omnidirectional mode, the prototype achieved a 107.07% bandwidth (0.92–3.04 GHz, $VSWR \leq 2.0$) with an XPD level better than 19.5 dB. In its directional mode, it achieved an impedance bandwidth exceeding 100% (1–3 GHz, $VSWR \leq 3.0$) with an XPD level greater than 20.9 dB. Minor deviations from this bandwidth performance occur at the low- and high-frequency ends, particularly for its edge elements. The array also exhibits scan invariance with a maximum deviation of 0.8 dB in its directional mode. The developed array presents a promising solution for passive sensing applications requiring UWB coverage, wide-angle coverage, and high-accuracy geolocation.

REFERENCES

- [1] Y. J. Guo and R. W. Ziolkowski, *Advanced Antenna Array Engineering for 6G and Beyond Wireless Communications*, 1st ed. Wiley, 2021.
- [2] T. C. Baum, R. W. Ziolkowski, K. Ghorbani, and K. J. Nicholson, "Investigations of a load-bearing composite electrically small Egyptian axe dipole antenna," *IEEE Trans. Antennas Propagat.*, vol. 65, no. 8, pp. 3827–3837, Aug. 2017.
- [3] F. Colone, F. Filippini, and D. Pastina, "Passive radar: past, present, and future challenges," *IEEE Aerosp. Electron. Syst. Mag.*, vol. 38, no. 1, pp. 54–69, Jan. 2023.
- [4] H. Wheeler, "Simple relations derived from a phased-array antenna made of an infinite current sheet," *IEEE Trans. Antennas Propagat.*, vol. 13, no. 4, pp. 506–514, Jul. 1965.
- [5] A. Neto and J. J. Lee, "Ultrawide-band properties of long slot arrays," *IEEE Trans. Antennas Propagat.*, vol. 54, no. 2, pp. 534–543, Feb. 2006.
- [6] Hansen, "Linear connected arrays [coupled dipole arrays]," *IEEE Antennas Wirel. Propag. Lett.*, vol. 3, pp. 154–156, 2004.
- [7] A. Neto and J. J. Lee, "'Infinite bandwidth' long slot array antenna," *IEEE Antennas Wirel. Propag. Lett.*, vol. 4, pp. 75–78, 2005.
- [8] J. P. Doane, K. Sertel, and J. L. Volakis, "A wideband, wide scanning tightly coupled dipole array with integrated balun (TCDA-IB)," *IEEE Trans. Antennas Propagat.*, vol. 61, no. 9, pp. 4538–4548, Sep. 2013.
- [9] E. Yetisir, N. Ghalichechian, and J. L. Volakis, "Ultrawideband array with 70° scanning using FSS superstrate," *IEEE Trans. Antennas Propagat.*, vol. 64, no. 10, pp. 4256–4265, Oct. 2016.
- [10] S. Kim and S. Nam, "Bandwidth extension of dual-polarized 1-D TCDA antenna using VMS," *IEEE Trans. Antennas Propagat.*, vol. 67, no. 8, pp. 5305–5312, Aug. 2019.
- [11] R. N. Paek, A. S. Brannon, and D. S. Filipovic, "Tightly coupled array of horizontal dipoles over a ground plane," *IEEE Trans. Antennas Propagat.*, vol. 68, no. 3, pp. 2097–2107, Mar. 2020.
- [12] Z. D. Wang, Y. Z. Yin, X. Yang, and J. J. Wu, "Design of a wideband horizontally polarized omnidirectional antenna with mutual coupling method," *IEEE Trans. Antennas Propagat.*, vol. 63, no. 7, pp. 3311–3316, Jul. 2015.
- [13] H. Liu, Y. Liu, W. Zhang, and S. Gao, "An ultra-wideband horizontally polarized omnidirectional circular connected Vivaldi antenna array," *IEEE Trans. Antennas Propagat.*, vol. 65, no. 8, pp. 4351–4356, Aug. 2017.
- [14] W. M. Dorsey, A. Stumme, K. M. Charipar, and N. A. Charipar, "3-D-printed circular array for WiMAX base station," *IEEE Antennas Wirel. Propag. Lett.*, vol. 18, no. 6, pp. 1159–1163, Jun. 2019.
- [15] Z. Wang, P. S. Hall, J. R. Kelly, and P. Gardner, "Wideband frequency-domain and space-domain pattern reconfigurable circular antenna array," *IEEE Trans. Antennas Propagat.*, vol. 65, no. 10, pp. 5179–5189, Oct. 2017.
- [16] J. T. Logan, W. M. Dorsey, and J. A. Valenzi, "Modular all-metal ultrawideband cylindrical array for multifunction operation," *IEEE Trans. Antennas Propagat.*, vol. 70, no. 10, pp. 9175–9183, Oct. 2022.